EpitopeMap exchange grant report:

Statistical View of Impacts of Surface-Modified Nanoparticles at Single Cell Level

Anna Hallerbach
anna.hallerbach@gmail.com
Chalmers Technical University

Introduction

Nanoparticles dispersed in biological fluids are rapidly covered by a tightly bound layer of proteins (and other biomolecules) — the 'protein corona' [2]. The nature and composition of the protein corona is dependent on nanoparticle characteristics (such as material, size, charge etc.) in ways that are currently being explored. In particular, carboxylated and amine-modified polystyrene nanoparticles (PS-NPs) of the same size, while based on the same polymer, exhibit different protein coronas [3]. Interestingly, these two types of nanoparticles also induce vastly different behavior once internalized by cells: The carboxylated PS-NPs do not affect the cell [4, 1], while the amine-modified PS-NPs induce cell death [5, 1], suggesting a role of the protein corona (and/or its intracellular evolution) in the response.

Within the host group, a theoretical framework has previously been developed for describing the behavior of nanoparicles (NPs) inside the cell, as well as their perturbations on organelles (e.g. mitochondria). The response of mitochondria is particular intriguing, as the mitochondria have been shown to be involved in the cell death that takes place due to the presence of the amine-modified PS-NPs [1, 5].

With this background, the goal of the current project was to describe mitochondria from a statistical point of view, in order to facilitate an assessment of the kinetics involved. Ultimately, knowing the kinetics could aid the understanding

of how the response of the two types of PS-NPs (the two types of protein coronas) come about. The proposed description of the mitochondria is based on the framework developed within the group which looks at the spatial correlation of distances between mitochondria. The difference between the original method and the method developed here is that mitochondria are defined pixel-based rather than object-based. To identify mitochondria, the image is segmented, divided into mitochondria and non-mitochondria pixels, semi-automatically.

The results, using the pixel-based approach, are supportive of the results from an object-based method, although it is computationally much more expensive.

Methods

Images: Images from cells from the A549 cancer cell line have been obtained using spinning disk confocal microscopy. This way stained organelles (e.g. mitochondria) and fluorescent nanoparticles (NPs) can be visualized and located. It is even possible to follow the uptake and the responses of the organelles to the NPs as a function of time. This results in 3-dimensional images over several time frames.

Segmentation of mitochondria: The goal in the pixel-based approach to quantify cell behavior is to focus only on one type of organelle, in this project mitochondria. The most straight forward approach is to divide the image into mitochondria and non-mitochondria pixels. This segmentation is done best in two steps, the first being the manual identification of the cell and the second the identification of the mitochondria via thresholding. Simply thresholding the complete image is not sufficient due to different intensity values of the cell, mitochondria and non-cell in different time frames and z-planes. It would result in either missing most mitochondria or including non-mitochondria and specifically non-cell parts in the analysis.

After segmentation of the mitochondria, the included area is smoothed to get a more realistic view. All pixels which fall into the segmented areas are considered in the further analysis. Examples of the identification of the cell can be seen in Figure 1 and an example of the segmentation of the mitochondria in Figure 2.

The segmentation of mitochondria is done according to the following algorithm:

1. Segmentation of cell

    i) Average image over all frames to reduce fluctuations in intensity values allowing for better identification of the cell

    ii) Define polygon around the cell

    iii) Allow for a margin of error

2. Segmentation of mitochondria

    i) Threshold each z-plane individually to include all mitochondria

    ii) Filling of holes of thresholded images

    iii) Closing of thresholded images

    iv) Opening of thresholded images

Spatial correlation of distances: The spatial correlation or pair correlation function requires to compute all pairwise distances of mitochondria pixels. This results in large amounts of distances and of required computer memory, therefore the distances could not all be stored. Hence, the distances were included in a histogram with very small bin size ($0.05\mu m$), resulting in $dist$. The bin edges can be considered as different radii r for further calculations. From this histogram the normalized distribution of distances $dist_n$ can be computed.

$$dist_n(r) = \frac{dist(r)}{\sum dist} \tag{1}$$

From Equation 1 the pair correlation function $g(r)$ (Equation 2) is calculated.

$$g(r) = \frac{dist_n(r)}{4\pi r^2 dr}, \tag{2}$$

where r is the radius of the sphere around the target mitochondria pixel and dr the bin size of the histogram.

Results

Segmentation of cells: The outline of the cell is defined manually as a polygon. In the images in Figure 1, which are averaged over the third dimension (z-planes),

the cell sets itself apart nicely from the rest of the image. The solid black line represents the polygon and the dashed line represents a margin of error which is included in the subsequent analysis.

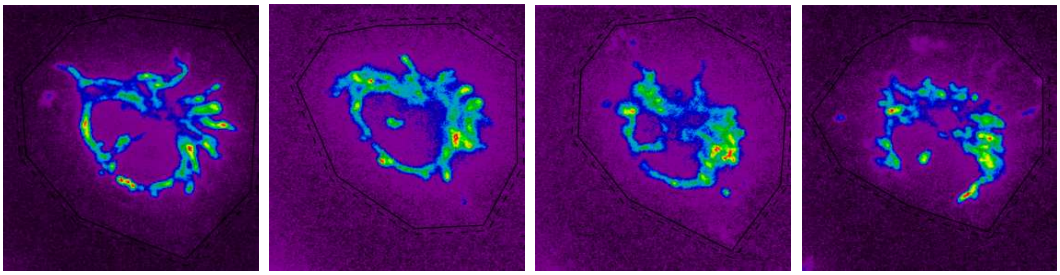

(a) 20 min (b) 45 min (c) 120 min (d) 180 min

Figure 1: Segmentation of the cell is done by fitting of a polygon around the cell (solid line) and allowing for a margin of error (dashed line). (a)-(d) show different time points in the analysis of the same cell.

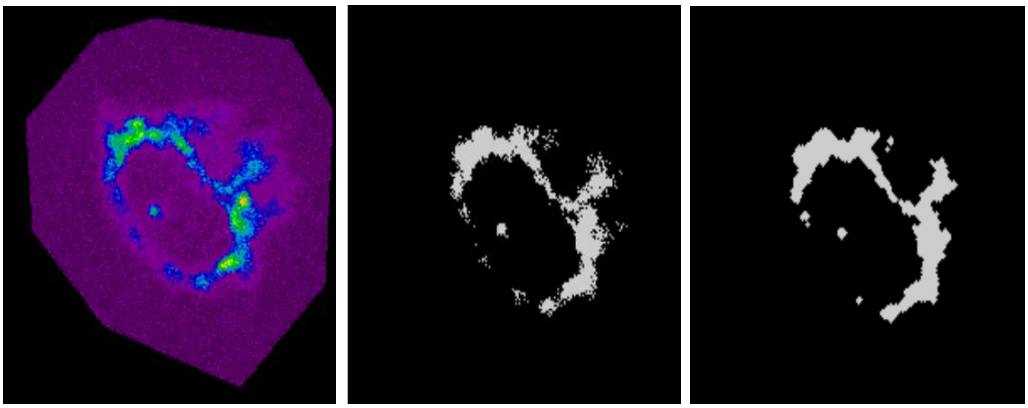

(a) After polygon fitting (b) After thresholding (c) After processing

Figure 2: Thresholding of mitochondria in the same cell as in Fig. 1. (a) shows only the segmented cell. (b) shows the thresholded image. (c) shows the image after smoothing. The pixels from (c) are used in further analysis as mitochondria.

Thresholding of mitochondria: An example of the thresholding can be viewed in Figure 2. For each cell the threshold has been determined manually for each z-plane. Thresholds range from $200 - 800$ as intensity value cut-offs. Applying only the simple threshold would result in Figure 2(b). Since it is obvious that

mitochondria should be more connected and smoother than in Figure 2(b) the previously described processing is applied resulting in Figure 2(c).

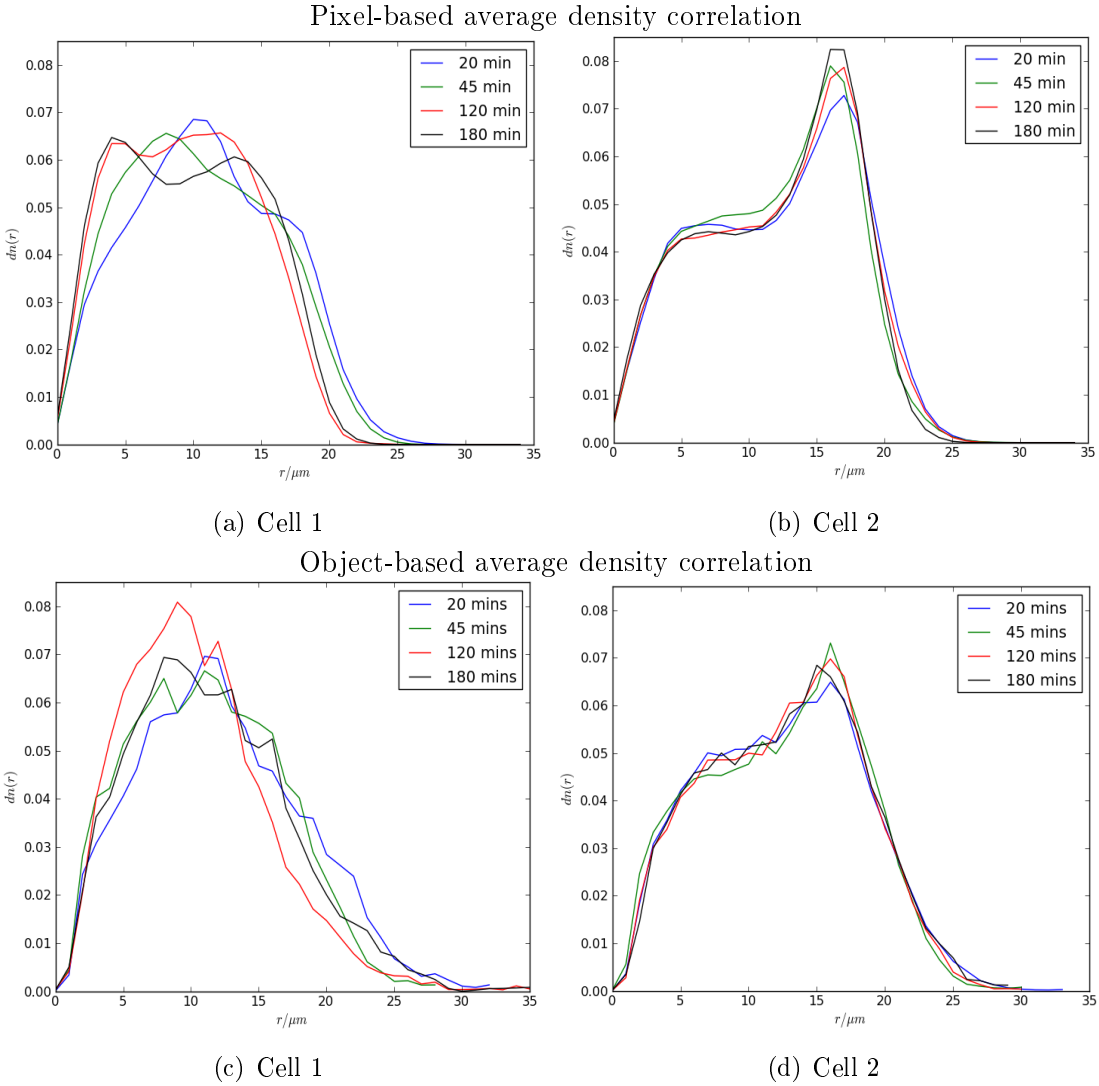

(a) Cell 1 (b) Cell 2

(c) Cell 1 (d) Cell 2

Figure 3: Normalized counts of pairwise distances for two different cells at different time points. (a) and (b) show results for the pixel-based approach and (c) and (d) for the object-based approach. (a) and (c) are the same cell as well as (b) and (d).

Spatial correlation of distances: Computing the spatial correlation of the mitochondria is computationally very expensive. After segmentation of the mitochondria there are roughly $24,000 - 50,000$ pixels in each frame which are mitochondria. That corresponds to roughly $300,000,000 - 1,000,000,000$ pairwise

distances which need to be computed. For each frame it takes about a day to sort the distances into a histogram which makes a total of about two to three weeks to complete the analysis of the whole image.

Figure 3 shows the normalized distribution of distances in two different cells obtained with both the pixel-based approach (Fig. 3(a) and 3(b)) and the object-based approach (Fig. 3(c) and 3(d)). It can be seen that the results are supportive of each other since not only the behavior of the graphs is the same but also the scale is almost the same.

Figure 4 shows $g(r)$, the pair correlation function of distances. It shows that most pixels are within $1\mu m$ from one another. It is interesting to note that in Figure 4(b) the scale for the different time points is nearly the same for the peak and even better aferwards.

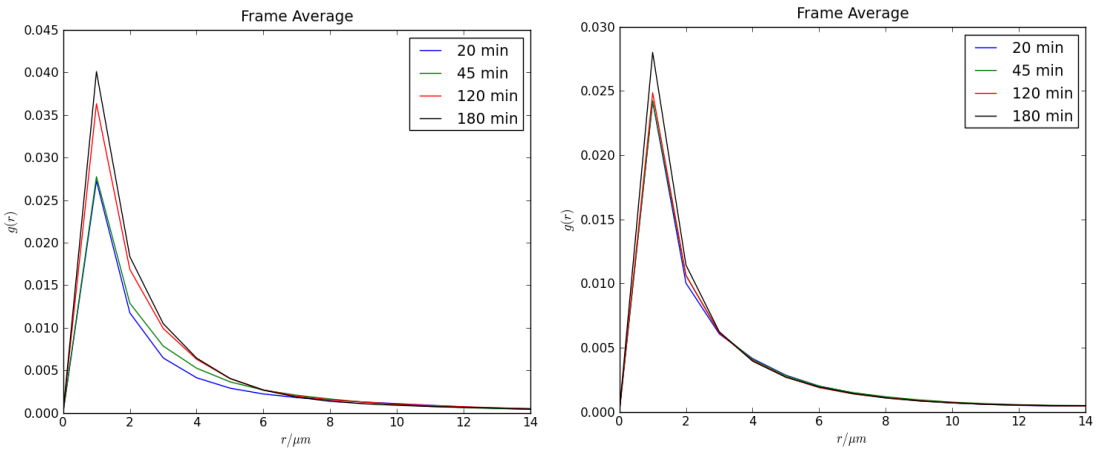

(a) Cell 1 (b) Cell 2

Figure 4: Pair correlation function, $g(r)$, for two different cells at different time points.

Figure 5 gives an impression of the accuracy of the average over frames. The graphs on the left show how much the average differs from one single frame and the right graph shows the development of the average for three different bins as more and more frames are taken into account for computing the average. 23 frames were considered in the analysis but as seen in the left graphs the average is stable after around 10-15 frames as the graphs are well inside a 5% margin.

Conclusion

Mitochondria have been successfully identified with the described two step segmentation process. The pixel-based approach to the analysis of organelles is in principle more correct, and, indeed, shows superior results compared to the object-based method, as seen in Figure 3. However, there is a large computational cost associated with the pixel-based method. As the object-based method gives similar results (apart from the larger fluctuations), which method to use should in the future be chosen based on a compromise between computational cost and precision.

Regardless, the appropriateness and limits of the object-based method has been properly assessed. With this background, it is now possible to find a detailed view of the effect of nanoparticles on mitochondria. In particular, the results can be used as a firm theoretical basis to describe the effects on the cell (or lack thereof) by the amine-modified and carboxylated PS-NPs, ultimately correlating this with their different protein coronas (and/or its intracellular evolution).

References

[1] M.G. Bexiga, J.A. Varela, F. Wang, F. Fenaroli, A. Salvati, I. Lynch, J.C. Simpson, and K.A. Dawson. Cationic nanoparticles induce caspase 3-, 7-and 9-mediated cytotoxicity in a human astrocytoma cell line. *Nanotoxicology*, (0):1–11, 2010.

[2] Tommy Cedervall, Iseult Lynch, Stina Lindman, Tord Berggård, Eva Thulin, Hanna Nilsson, Kenneth A. Dawson, and Sara Linse. Understanding the nanoparticle–protein corona using methods to quantify exchange rates and affinities of proteins for nanoparticles. *Proceedings of the National Academy of Sciences*, 104(7):2050 –2055, February 2007.

[3] Martin Lundqvist, Johannes Stigler, Giuliano Elia, Iseult Lynch, Tommy Cedervall, and Kenneth A. Dawson. Nanoparticle size and surface properties determine the protein corona with possible implications for biological impacts. *Proceedings of the National Academy of Sciences*, 105(38):14265 –14270, 2008.

[4] Anna Salvati, Christoffer Åberg, Tiago dos Santos, Juan Varela, Paulo Pinto, Iseult Lynch, and Kenneth A. Dawson. Experimental and theoretical com-

parison of intracellular import of polymeric nanoparticles and small molecules: Towards models of uptake kinetics. *Nanomedicine: Nanotechnology, Biology and Medicine*, March 2011.

[5] T. Xia, M. Kovochich, M. Liong, J.I. Zink, and A.E. Nel. Cationic polystyrene nanosphere toxicity depends on cell-specific endocytic and mitochondrial injury pathways. *ACS nano*, 2(1):85–96, 2007.

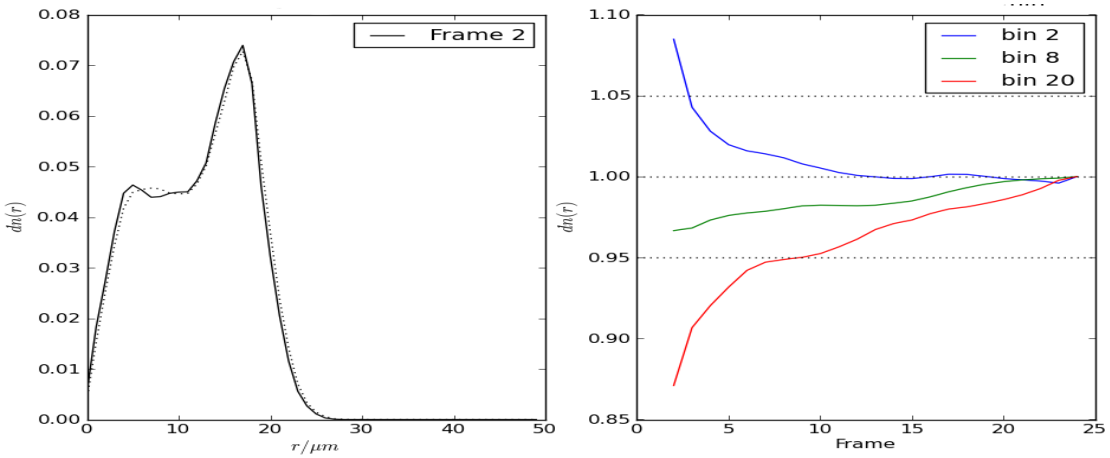

(a) 20 mins

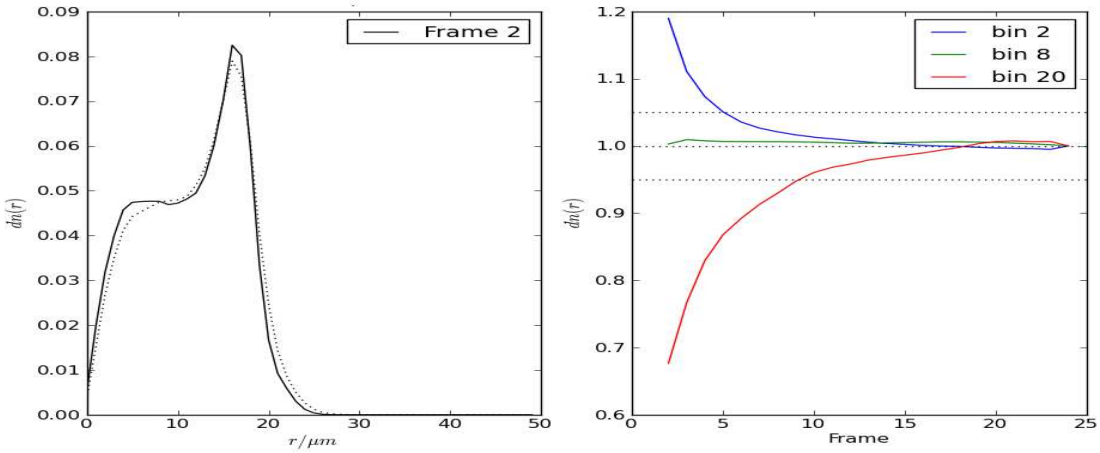

(b) 45 mins

Figure 5: Frame averaged results are reliable within a 5% margin (dotted lines at 1.05 and 0.95) as seen in the right graph. It shows how the average changes for three different bins when more frames are added into the average. The left graphs show how the average is different with respect to one single frame. The images are all from same cell as in Fig. 3(b) and for two different time points, (a) 20 mins and (b) 45 mins.